TacPrint: Visualizing the Biomechanical Fingerprint in Table Tennis

Jiachen Wang, Ji Ma, Zheng Zhou, Xiao Xie, Hui Zhang, Yingcai Wu, and Huamin Qu

***Abstract*—Table tennis is a sport that demands high levels of technical proficiency and body coordination from players. Biomechanical fingerprints can provide valuable insights into players' habitual movement patterns and characteristics, allowing them to identify and improve technical weaknesses. Despite the potential, few studies have developed effective methods for generating such fingerprints. To address this gap, we propose TacPrint, a framework for generating a biomechanical fingerprint for each player. TacPrint leverages machine learning techniques to extract comprehensive features from biomechanics data collected by inertial measurement units (IMU) and employs the attention mechanism to enhance model interpretability. After generating fingerprints, TacPrint provides a visualization system to facilitate the exploration and investigation of these fingerprints. In order to validate the effectiveness of the framework, we designed an experiment to evaluate the model's performance and conducted a case study with the system. The results of our experiment demonstrated the high accuracy and effectiveness of the model. Additionally, we discussed the potential of TacPrint to be extended to other sports.**

***Index Terms*—Data transformation, biomechanical data, machine learning.**

I. Introduction

TABLE tennis is a challenging and competitive sport in which players use various techniques to respond to their opponent's strokes (a stroke represents a player hitting the ball once) during a match. The success of these techniques largely depends on the player's body coordination [65]. For instance, when playing a forehand topspin, a commonly used technique, the speed and spin of the ball can be affected by the rotation rate and angle of the player's trunk and shoulders [23]. To help players optimize their body coordination, extensive studies have been conducted to explore the biomechanics of table tennis. Researchers use sensors or motion capture devices with inertial measurement units (IMU) to collect players' biomechanical data which includes acceleration, angle, etc. With the data, these studies focus on unraveling the complex interactions between various body segments and their impact on the execution of specific techniques. However, few studies have investigated the biomechanical fingerprint of an individual player.

We define the biomechanical fingerprint of a player as the characteristic set of biomechanics that summarize and reflect his/her habitual movement patterns. These patterns can facilitate performance enhancement, personalized training development, injury prevention, talent identification, as well as innovation in training methods and techniques. However, obtaining the biomechanical fingerprint is a non-trivial issue because each player possesses a unique biomechanical profile that characterizes the complex interplay of body movements and performances. Developing a comprehensive method to accurately capture and characterize the unique aspects of each player's biomechanical fingerprint poses a significant challenge. Researchers have tried to use 177 diverse indicators to specify the fingerprint of rowers [18]. While this method is effective, it is difficult and time-consuming to extend to our field since the game rules of table tennis are quite different from those of rowing and we need to assess each indicator to determine whether it can be used for specifying the fingerprints of table tennis players. To address these issues, we leverage machine learning and visualization techniques to automatically generate and visually investigate the biomechanical fingerprints of table tennis players.

Machine learning techniques have opened up new avenues for the analysis of biomechanical data in sports [37], [38], [39]. In table tennis, established techniques such as Support Vector Machine (SVM) [21] and Long-short Term Memory (LSTM) [22] have been used to support research in various areas such as stroke recognition [4], [61] and ball speed and spin estimation [3], [49]. Besides, visualization techniques have also successfully driven the development of biomechanics in sports. [2]. In table tennis, an IoT + VA framework [49] has been proposed to facilitate investigating biomechanical data in training. Despite the widespread application of machine learning and visualization techniques in table tennis, investigating biomechanical fingerprints using these techniques still poses three challenges: feature comprehensiveness, model interpretability, and result intuitiveness.

First, existing studies can extract highly representative features from biomechanics data since they have achieved high performance in various tasks [3], [4], [61]. However, these

Manuscript received 1 October 2023; revised 1 December 2023; accepted 22 December 2023. Date of publication 15 April 2024; date of current version 19 June 2024. This work was supported by NSFC under Grant U22A2032, in part by the Key "Pioneer" R&D Projects of Zhejiang Province under Grant 2023C01120, and in part by the HK RGC GRF 16210321. Recommended for acceptance by N. Elmqvist, S. Liu, and V. Pascucci. *(Corresponding author: Xiao Xie.)*

Jiachen Wang, Ji Ma, and Yingcai Wu are with the State Key Lab of CAD&CG, Zhejiang University, Hangzhou 310027, China (e-mail: wangjiachen@zju.edu.cn; zjumaji@zju.edu.cn; ycwu@zju.edu.cn).

Zheng Zhou, Xiao Xie, and Hui Zhang are with the Department of Sports Science, Zhejiang University, Hangzhou 310027, China (e-mail: zheng.zhou@zju.edu.cn; xxie@zju.edu.cn; zhang_hui@zju.edu.cn).

Huamin Qu is with the Department of Computer Science and Engineering, Hong Kong University of Science and Technology, Hong Kong (e-mail: huamin@cse.ust.hk).

This article has supplementary downloadable material available at http://doi.org/10.1109/TVCG.2024.3388555, provided by the authors.

Digital Object Identifier 10.1109/TVCG.2024.3388555

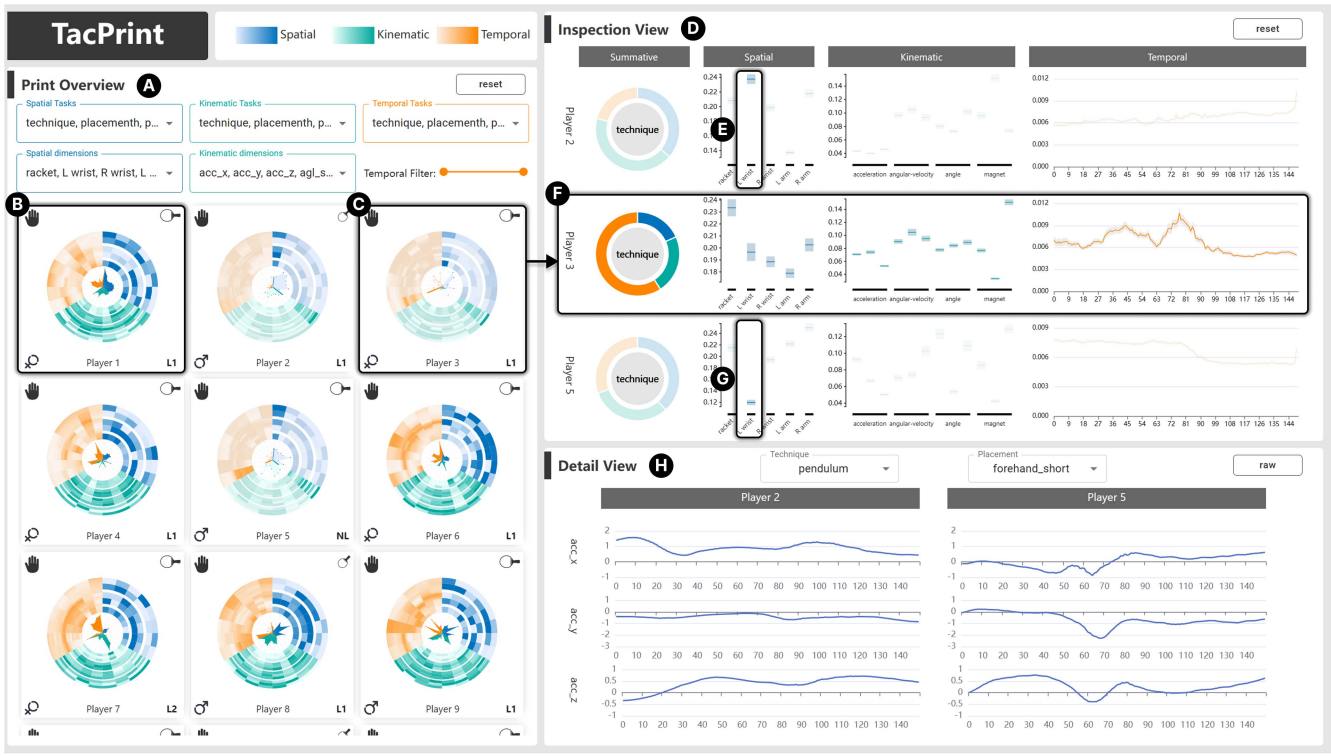

Fig. 1. The interface of the system. A print overview (A) presents the visualized fingerprints (B) of various players. An inspection view (D) presents the detailed attention information (F) selected in the print overview (C). A detailed view (H) presents the original biomechanical data of the dimensions selected in the inspection view (E, G).

studies use different models for different tasks. If we focus on one of these models, the features are not comprehensive enough since the features may only work on particular tasks, representing limited data features. If we include all of the models, it is difficult to fuse all features due to the heterogeneity of feature vectors. How to extract comprehensive features to generate the fingerprint is a challenge. Second, state-of-the-art machine learning techniques, such as LSTM, are inherently non-linear, making it difficult to interpret the mechanisms and results of these models. The fingerprints generated based on such techniques will naturally be confusing. Additionally, coaches and players intrinsically have difficulties in understanding machine learning models. They would doubt the reliability of the generated fingerprints. How to increase the interpretability and credibility of the model is also a challenge. Third, the fingerprints generated by machine learning techniques are abstract. They are often represented by high-dimensional vectors or tensors. While the numerical representation can be accurate in capturing players' characteristics, analyzing such data is struggling. How to effectively visualize these fingerprints to support efficient investigation is challenging.

To address these challenges, we worked extensively with professional analysts serving the Chinese national table tennis team to introduce TacPrint, a framework for generating a biomechanical fingerprint for each player. The framework consists of four components, namely, data recombination (Fig. 3(A)), feature generation (Fig. 3(B)), feature fusion (Fig. 3(C)), and print embodiment (Fig. 3(D)). Data recombination transforms

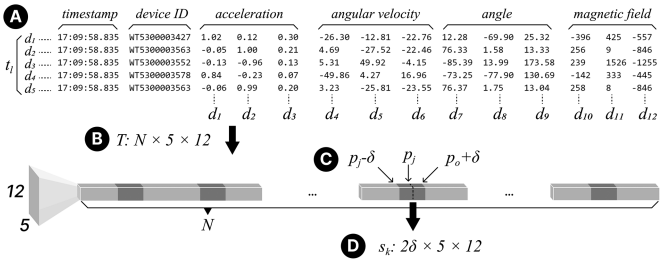

Fig. 2. The data in this work. (A) is the raw data of one timestamp. (B) is the time series data transformed from (A). (C) presents the timestamp of a peak and the range of a serve. (D) is the shape of the final serve data.

the serve data into three forms. Feature generation generates summative features, spatial features, kinematic features, and temporal features based on the transformed data. After that, feature fusion integrates all features into one fingerprint, and print embodiment visualizes the fingerprint for further analysis. To solve the first challenge, we constructed a new model based on a bidirectional LSTM network (BiLSTM) [19]. The performance of the model was better than existing models in various tasks (i.e., the recognition of technique, placement, spin type, player, holder type, profession level, and gender). We can only use this model to acquire comprehensive features in feature generation. To solve the second challenge, we employed the attention mechanism by incorporating four attention layers. This enabled us to unveil the model's attention from four perspectives, which served as integral components of the fingerprints. To

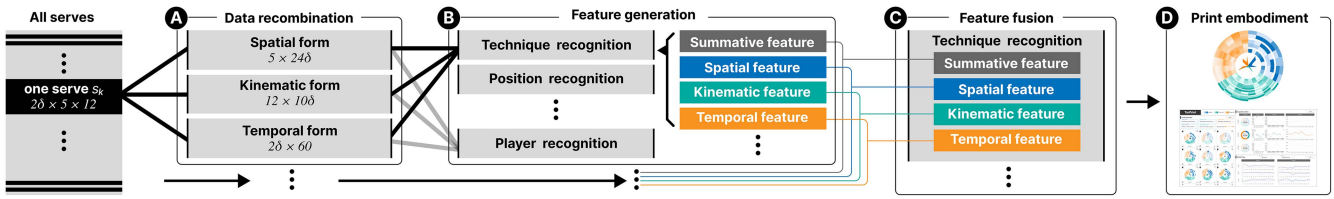

Fig. 3. The framework of TacPrint. The data recombination component (A) transforms the data of a serve into three forms. The feature generation component (B) generates the biomechanical features from four perspectives. The feature fusion component (C) combines all kinds of features to construct a biomechanical fingerprint. The print embodiment component (D) visualizes the fingerprints with an interactive system.

solve the third challenge, we designed a novel visualization for biomechanical fingerprints. Based on the design, we developed an interactive visualization system to support the exploration and investigation of fingerprints. We used the system to discover several valuable insights into the players' biomechanical characteristics. The insights were validated by the players themselves. The framework is generalizable for various sports, such as tennis, basketball, and soccer, as long as the input is biomechanical data collected by IMU devices. The contributions are as follows.

- We defined the concept of biomechanical fingerprints.
- We introduced a framework called TacPrint for generating the biomechanical fingerprints of table tennis players, which can be generalized for other sports.
- We developed an interactive visualization system to support the analysis of biomechanical fingerprints.
- We designed an experiment to verify the models within TacPrint and discovered valuable insights with two cases.

II. Related Works

In this section, we reviewed research on biomechanics in table tennis, machine learning in sports biomechanics, and sports visualization.

A. Biomechanics in Table Tennis

Biomechanics research in table tennis aims to examine the mechanical characteristics of players' bodies as they execute various techniques [32]. For example, Iino and Kojima [24], [25] explored the energy generation mechanism of the upper limb during the execution of the topspin forehand. Building on these studies, Iino et al. [28] found that the lower limb has a significant impact on upper limb performance, resulting in extensive investigations of the role of the lower limb in topspin forehand execution [20]. Additionally, researchers have explored the biomechanical properties of other body parts, including the trunk [26], [27] and the sole [16], [31]. A comprehensive review of these studies is available [55]. The insights from these investigations can help coaches develop training regimes to improve players' performance.

However, these studies endeavor to discover common characteristics by examining the biomechanical data of multiple players. The specific characteristic of an individual player, also known as the biomechanical fingerprint in this work, has not been fully studied yet. Gravenhorst et al. selected 177 performance metrics as the fingerprint of rowers to characterize their technique styles [18]. While this method can help coaches find the most suitable players for crews, it is time-consuming since researchers have to examine considerable metrics. Besides these metrics are not compatible with other sports. To fill this gap, we propose TacPrint, a fingerprint generation framework based on existing biomechanical findings in table tennis.

B. Machine Learning in Sports Biomechanics

In recent years, machine learning techniques have assumed an increasingly vital role in the analysis of biomechanics data in sports. One of the most popular machine learning methods is SVM [21]. Both Lu et al. [37] and Blank et al. [4] employed an SVM-based classifier for action recognition. Wang et al. [52] used a PCA+SVM method to investigate the differences between the elite and amateurs. To achieve better performance, non-linear models are used for analysis. For example, Ma [38] constructed a two-layer neural network to recognize movements in basketball. Wang et al. [49] tried to use LSTM [22] to classify different techniques and positions of table tennis strokes. Other methods such as Random Forest [6], XGBoost [7], LightGBM [30], etc., have also been applied to action recognition or indicator estimation tasks. These studies present the advantage of machine learning methods in extracting players' biomechanical features in various sports. This advantage suggests the potential to generate players' fingerprints by using learning-based methods.

However, the biomechanical features extracted by existing learning-based methods are not comprehensive enough for generating fingerprints since each of them performs well on particular tasks. It is challenging to combine all of the heterogeneous features of various models. A comprehensive method that is powerful enough for various tasks is necessary. Moreover, the features of the non-linear models are difficult to interpret. Analysts cannot understand the physical meaning of abstract feature vectors. To solve these issues, we refer to existing studies and propose TacPrint, a comprehensive and interpretable learning-based method for generating players' biomechanical fingerprints.

C. Sports Visualization

Recent years have witnessed an increase in the visualization methods for sports analytics [15], [43], [64]. Time series visualizations are commonly used to display the spatiotemporal features of competitions. For example, line charts and histograms are popular choices for presenting the variation of score-related statistics [42], [46] and players' performance indicators [1], [17], [29] in soccer and basketball. Trajectories are also commonly

used to display players' movements [9], [36], [48]. Besides, researchers also introduced many novel time-series visualizations. Wu et al. [60] introduce a formation flow to visualize the dynamics of formation transformation in soccer. Chen et al. [8] designed GameFlow to present game scores along with team information in basketball. Wongsuphasawat and Gotz [56] proposed Outflow to display events and outcomes during competitions. Since the biomechanical data is time series data, we used time series visualizations such as line charts to visualize the temporal features within a biomechanical fingerprint.

Giyph-based visualizations are also widely used in sports visualization to present patterns within high-dimensional sports data, including key events, game scores, action attributes, performance indicators, etc. For example, in soccer, both Rusu et al. [45] and Stein et al. [47] designed a novel glyph to compare players' performances during matches. Xie et al. [62] used a pitch-based glyph to present the dynamic passing patterns vividly. In basketball, Wu et al. [59] introduced a glyph to encode off-ball movement. The glyphs are plotted on a two-dimensional coordinate system to provide an overview. In rugby, Legg et al. [33], [34] and Chung et al. [10], [11] designed player-based glyphs to facilitate analysis of game events and statistics. In tennis, Polk et al. [44] used a ball-based glyph to intuitively display score information. In table tennis, considerable efficient glyphs have been introduced to encode multivariate stroke attributes and indicators by Wu et al. [60] and Wang et al. [49], [50], [51]. Wu et al. [57], [58] designed two glyphs for technical attributes of badminton and tennis, respectively. While existing glyphs cannot be directly applied to present players' biomechanical fingerprints, these studies provided valuable design guidelines for us. We referred to these studies and the design guidelines summarized by Borgo et al. [5] to design a novel glyph to illustrate players' fingerprints.

III. Background

This section introduces the domain experts, the knowledge about table tennis, the data collection procedure, and the data processing methods.

A. Domain Experts

In this work, we collaborated with an expert from the Chinese national table tennis team. He has served as an analyst for the team since 2003. He also has rich training and competition experiences and was a Level-1 table tennis player, international referee, Level-1 coach, and coach with an A-Level certificate in Germany. His research focuses on match analysis and training analysis in various sports, including table tennis, badminton, soccer, etc. We held weekly meetings with him to embody table tennis players' fingerprints based on the biomechanical data.

B. Table Tennis & Serve

Table tennis is a racket sport that involves two players (or four in doubles) hitting a ball back and forth using rackets in a rally. Players must utilize a range of techniques to respond to their opponent's strokes in order to win points. A rally is won by a player when he/she hits the last stroke and his/her opponent fails to successfully return the stroke. Due to the sequential property, the most important stroke of a rally is the first stroke, namely, the serve [65]. According to our expert, the player who serves has an advantage over his/her opponent since he/she can control the pace of the rally. Players tend to prioritize improving their serving abilities over other techniques and aim to develop distinctive serving styles. Notably, some players intentionally utilize similar movements to execute different serve techniques, which can deceive their opponents during matches. Consequently, compared with other techniques, serve contains more representative characteristics. Inspired by this condition, we, together with our expert, decided to generate a player's fingerprint based on the biomechanical data collected during the player's serve.

C. Data Description

We collected the biomechanical data of 12 professional table tennis players during their serving by using IMU devices. The data were further processed to fit our framework.

1) Device Configuration: We used IMU devices, *WT901WIFI* developed by *WitMotion*[1] to collect the data. Each device measures $(51\times36\times15)mm$ in size and weighs $20\,g$, equipped with a tiny battery (3.7 V–260 mAh). It contains multiple inertial measurement units that can sense the acceleration, angular velocity, angular acceleration, and magnetic field in the x-y-z dimensions (twelve dimensions in total). The detailed parameters of the devices are shown in Table I. The devices came with a complementary data collection system that supports data synchronization, device configuration, and sensor calibration. Before data collection, we put all devices on the table. After we opened them, the system automatically synchronized the internal clock of each device. Then we performed the calibration function in the system to calibrate all inertial sensors. To reserve the most details of players' movements, we set the sampling frequency of the devices to $100\,Hz$ in the system.

2) Collection Procedure: We recruited 12 professional players (6 males and 6 females), including 1 National Level player, 10 Level-1 players, and 1 Level-2 player. Three of them used penhold grips and others used shakehand grips. All of them have played table tennis for more than 12 years. Each player was compensated with $10 for participating in the data collection for an hour. In the beginning, we bound the devices to a player's joints. We selected the player's upper limbs since during the serve, players' lower limbs must be stable enough to provide accurate power [65]. According to previous works, the devices were fixed to the right arm, right wrist, left arm, left wrist, and the end of the racket [3], [49]. Subsequently, each player underwent three distinct stages where they were required to serve the ball using three different techniques, namely, pendulum, reverse, and hook, as outlined in Table II. Different techniques would lead to different types of spin (i.e., top and down). Within each stage, the player had to serve the ball to six different placements (3 horizontal placements $\times$ 2 vertical placements) (Table II).

[1][Online]. Available: https://www.wit-motion.com/

TABLE I
THE RANGE AND THE ACCURACY OF THE IMU DEVICES

	Acceleration	Angular velocity	Angle	Magnetic field
Range	$\pm 16g$	$\pm 2000^\circ/s$	X,Z:$\pm 180^\circ$ Y:$\pm 90^\circ$	$\pm 3Guass$
Accuracy	$0.5mg/LSB$	$0.061(^\circ/s)/LSB$	$0.0055^\circ/LSB$	$0.0667mG/LSB$

TABLE II
THE VARIABLES WITHIN THE DATA COLLECTION PROCESS

Class name	Number of labels	List of attribute
Player	*12*	Player 1, ..., Player 12
Gender	*2*	Man (*6*), Woman (*6*)
Profession	*3*	NL (*1*), L1 (*10*), L2 (*1*)
Grip	*2*	Shakehand (*9*), Panholder (*3*)
Technique	*3*	Pendulum, Reverse, Hook
Spin	*2*	Top, Down
$Placement_h$	*3*	Forehand, Middle, Backhand
$Placement_v$	*2*	Short, Long

Furthermore, for each placement, the player had to serve the ball repeatedly 20 times using the same technique. After completing each placement, the data collected by devices were saved in an independent file and the player was given a one-minute break, while a five-minute break was provided after completing a stage. During the data collection process, we also recorded the validity of each serve. This was important because some serve might go out of bounds or hit the net, and would not be considered valid.

3) Data Preparation: Each player's serve data was recorded in 18 text files (3 techniques $\times$ 3 horizontal placements $\times$ 2 vertical placements) as described in Section III-C2. We use $A = (S_1, S_2, \ldots, S_{18})$ to denote the data of all serves of a player. Each text file recorded the biomechanical data of a player when he/she served the ball with a particular technique to a particular placement. As Fig. 2(A) shows, each row of the file recorded one data frame from a device which included the timestamp, the device ID, and the acceleration, angular velocity, angular acceleration, and magnetic field in the x-y-z dimensions. We first transformed the text data into time-series data $T = (t_1, t_2, \ldots, t_L)$, where L is the duration of each file and $t_l, l \in [1, L]$ denotes the data of each timestamp. t_l contains the data from five IMU devices, namely, $t_l = (u_1, u_2, \ldots, u_5)$ (Fig. 2(A)). The data of each IMU device, $u_m, m \in [1, 5]$, contains the signal value of the twelve dimensions, namely $u_m = (d_1, d_2, \ldots, d_{12})$, and $d_n, n \in [1, 12]$ keeps two decimal places. The transformed shape of the time-series data is as Fig. 2(B) shows.

After the data transformation, we extracted the valid biomechanical data of all serves $S_i = (s_1, s_2, \ldots, s_{20}), i \in [1, 18]$ within a file. According to our observation, When players execute a serve, there are significant and sudden changes in their biomechanical indicators, such as the acceleration and the angle, resulting in noticeable peaks in the collected data. Therefore, we first refer to the method in [4] to detect the meaningful peaks representing serves in the data. We chose the acceleration signals (i.e., d_1, d_2, d_3 in Fig. 2(A)) to detect peaks because peaks in these dimensions are more representative than others. We first calculated the sum of squares for the dimensions to magnify peaks. Then, we use the *signal.find_peaks* function in *SciPy*[2] to detect the meaningful peaks. In this way, we found the timestamp of all meaningful peaks $P = (p_1, p_2, \ldots, p_J)$ (Fig. 2(C)), where J is the number of peaks. Then, we set a δ to extract the data around each peak $p_j, j \in [1, J]$ as the data of a serve. Specifically, each serve starts from $p_j - \delta$ and ends at $p_j + \delta$, namely, $s_k = \{t_l | l \in [p_j - \delta, p_j + \delta]\}, k \in [1, 20]$. The shape of s_k is a three-dimensional tensor as shown in Fig. 2(D).

IV. METHOD

In this section, we introduce the problem definition, the design requirements, and the detailed architecture of TacPrint.

A. Problem Definition

In this work, we used learning-based methods to generate biomechanical fingerprints given the outstanding performance of machine-learning models in various domains [12], [13], [63]. A straightforward solution is training an end-to-end model that takes the biomechanical data as input and outputs the fingerprints. However, defining the output format and annotating players' fingerprints for training is challenging since we did not know the ground truth about fingerprints. Therefore, we decided to use the features extracted by models to construct the fingerprints.

B. Design Requirements

We organized our experts' considerations about biomechanical fingerprints and summarized the following design requirements.

- *R1: Temporal features:* Temporal features present the pace style of a player. For example, some players serve with a clean and efficient motion, which results in a fast serve pace for them. On the contrary, some players' serve motion may last for a long time since they need to include some deceptive moves to confuse their opponents. The pace style can affect the opponents' strategy when receiving the serve, which is important during matches. Therefore, a fingerprint should incorporate features of the time.
- *R2: Spatial features:* Spatial features present the body coordination style of a player. Each player has a unique body coordination style. For example, some players have the most noticeable changes in their right wrist motion when serving the ball to different placements. Besides,

[2][Online]. Available: https://scipy.org/

Some players may change their left wrist motion when serving the ball with different techniques. The body coordination style reflects the key body joints of each player, which is important information during training. Therefore, a fingerprint should incorporate features of body joints.

- *R3: Kinematic features:* Kinematic features present the force style of a player. This style can be characterized by kinematic metrics, such as acceleration, angular velocity, etc. For example, some players have strong hitting force, which can be reflected by a larger acceleration measurement. Besides, some players have a strong explosive force, which can be reflected in more dramatic changes in angular velocity and acceleration. The force style is also an important message during training. Therefore, a fingerprint should incorporate features of kinematic metrics.
- *R4: Summative features:* Summative features summarize the importance of different features (i.e., **R1**, **R2**, and **R3**). For example, some players' coordination styles can represent their movement patterns and characteristics better than force styles. Their spatial features are more important than their kinematic features. While a fingerprint should provide as many kinds of features as possible, it should also enable experts to quickly grasp the most important features. Therefore, a fingerprint should incorporate summative features summarizing the importance of other features.
- *R5: Feature comprehensiveness:* Our approach uses a learning-based method, which means that the features extracted by the model can vary depending on the specific tasks at hand. For instance, when the model identifies serving techniques and positions, the extracted features will naturally differ. Additionally, the features extracted from the serve data of different players can also exhibit variations. Hence, it is crucial to thoroughly consider features under different circumstances when generating fingerprints.
- *R6: Feature visualizations:* Features in our model are typically represented as vectors, making it challenging for experts to comprehend. This becomes particularly overwhelming when a fingerprint contains diverse types of features. To address this issue, it is essential to develop efficient visualization methods that can help experts analyze fingerprints effectively.

C. Framework Overview

According to the design requirements, we constructed TacPrint, a framework for generating players' biomechanical fingerprints. The input is the biomechanical data of all serves of a player. The output is the visualization of his/her biomechanical fingerprint. TacPrint consists of four components: data recombination (Fig. 3(A)), feature generation (Fig. 3(B)), feature fusion (Fig. 3(C)), and print embodiment (Fig. 3(D)). First, data recombination takes each single serve s_k as input and transforms it into three forms, namely spatial form, kinematic form, and temporal form (**R1, R2, R3**). Then, feature generation computes corresponding features based on the data from data recombination by using various models (**R5**). Moreover, this component also computes additional summative features (**R4**). Afterward, feature fusion merges all feature data according to particular models, and fuses them into one fingerprint (**R5**). Finally, print embodiment visualizes the fingerprint and provides an interactive system for exploration and analysis (**R6**).

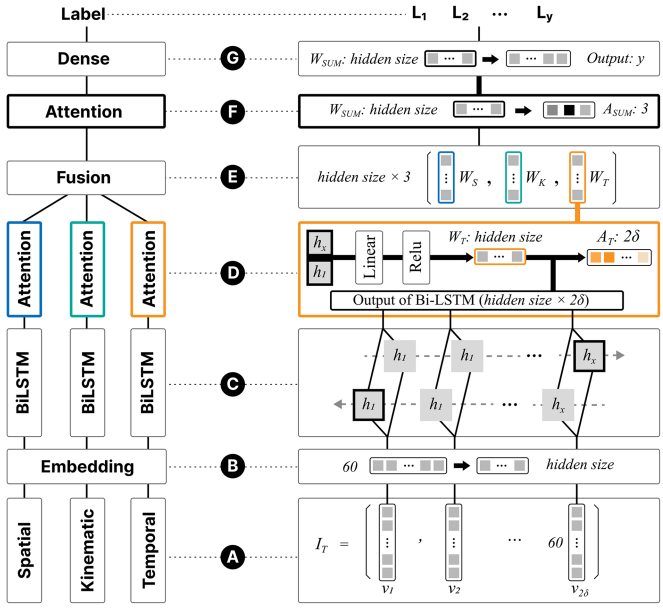

Fig. 4. The model architecture of the feature generation component. The data (A) first goes through an embedding layer (B) and is fed to three BiLSTM networks (C) with attention layers (D). The generated context vectors are fused in a fusion layer (E) and further fed to an additional attention layer (F). Finally, a dense layer (G) is used to output the label.

D. Data Recombination

Given the three types of features in **R1**, **R2**, and **R3**, we designed the data recombination component to transform the data into the spatial form, kinematic form, and temporal form, respectively (Fig. 3(A)). Specifically, for the three-dimensional tensor, s_k ($2\delta \times 5 \times 12$), we transformed it into three kinds of two-dimensional tensors. In the spatial form, we concatenated t_l (5×12) in s_k. The shape of this form was 5×24 δ. In the kinematic form, we first transposed t_l in s_k. The shape of the transposed t_l was 12×5. Then, we concatenated the transposed t_l. The shape of this form was 12×10 δ. In the temporal form, we concatenated d_m (1×12) in t_l. The shape of this form was $2\delta \times 60$. The shapes of the three data forms are presented in Fig. 4.

E. Feature Generation

Based on the three forms of data, feature generation aims to generate three kinds of features. Wang et al. [49] have tested various models for their performance in technical attribute recognition. However, in our conditions, these models did not meet our performance expectations since we not only needed them to accurately identify technical attributes but also to recognize additional information to ensure **R5**. Due to the powerful performance of recurrent neural networks in sequential data, we referred to BiLSTM [19] to improve the model performance.

Compared to regular LSTM, BiLSTM captures both past and future context, which leads to better performance. Additionally, the hidden states within BiLSTM are difficult for experts to understand. To solve this issue, we added the attention mechanism to BiLSTM since it has been used for model explanation in considerable cases [35], [40], [54].

The overall structure of the model in this component is displayed at the left of Fig. 4. We use I_S, I_K, and I_T to denote the model input in the three forms and take the temporal form as an example to demonstrate the details of the model. In Fig. 4(A), I_T is split into 2δ vectors, namely $I_T = \{v_1, \ldots, v_{2\delta}\}$. The length of each vector $v_a, a \in \{1, 2\delta\}$ is 60. v_a is fed to an embedding layer (Fig. 4(A)). The embedding layer is shared by I_S and I_K. It embeds v_a into v'_a whose length is $hiddensize$. After that, v'_a is fed to a BiLSTM [19] sequentially (Fig. 4(C)). In the attention layer (Fig. 4(D)), the final hidden states (h_1 and h_x) of both the forward and reverse LSTM networks are combined by vector summation as the attention generation key. The key is then passed through a linear layer with a Rectified Linear Unit (ReLU) activation function. This process generates the attention weights of the temporal form, W_T. The length of W_T is $hiddensize$. With W_T, we can obtain the attention vector A_T by implementing matrix multiplication between W_T and the output of BiLSTM whose shape is ($hiddensize \times 2\delta$). The attention weights (W_S, W_K) and vectors (A_S, A_K) of the other two forms are generated in the same way. In Fig. 4(E), W_S, W_K, and W_T are combined and fed to an additional attention layer to obtain the summative attention weights W_{SUM} and vector, A_{SUM}(Fig. 4(F)). The structure of this attention layer is the same as the former one and the key is W_T. Finally, W_{SUM} is fed to a dense layer and transformed to a vector with a length of the number of labels (Fig. 4(G)).

In this way, we can obtain the spatial feature (A_S), the kinematic feature (A_K), the temporal feature (A_T), and the summative feature (A_{SUM}). To ensure comprehensiveness (**R5**), this model is trained for 8 attribute recognition tasks suggested by our experts. As Table II shows, the tasks include the recognition of players ($Player$), gender ($Gender$), levels of the profession ($Profession$), grip styles ($Grip$), serve techniques ($Technique$), ball spin types ($Spin$), horizontal ball positions ($Placement_h$), and vertical ball positions ($Placement_v$). According to our experts, these attributes are the most important information for identifying a player's biomechanical characteristics.

F. Feature Fusion

Feature fusion aims to combine various features to produce a comprehensive fingerprint (**R5**). The attention vector of one serve is biased. However, preserving the vectors of all serves can overwhelm experts. Therefore, for each model, we calculated the average attention vectors of the four kinds of features based on the corresponding attention vectors of all serves. In this way, we used 32 (4 features $\times$ 8 models) average attention vectors to construct a fingerprint of a player. In addition, we also calculated the confidence interval of each value within the average attention vectors.

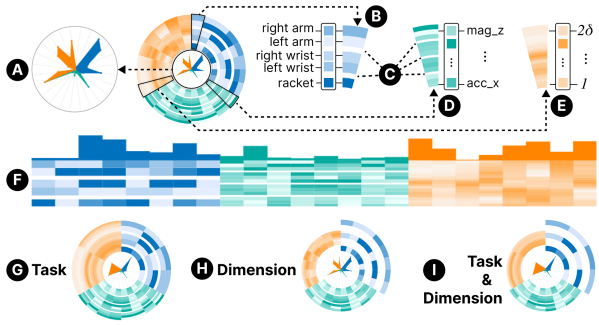

Fig. 5. The encoding of the glyph. (A) is a radar chart encoding the summative feature. (B), (D), and (E) use split arcs with heat maps to encode the spatial feature, the kinematic feature, and the temporal feature, respectively. (F) is an alternative to the glyph. (G), (H), and (I) are the fingerprints under different filtering conditions.

G. Print Embodiment

Print embodiment provides effective visualizations for experts to analyze fingerprints (**R6**). We designed a customized glyph to encode the fingerprints. The glyph can reveal the similarities and differences between multiple fingerprints. We further developed a visual analytics system to help experts discover the latent patterns within the fingerprints. The details about the glyph are presented in Section V.

V. Visualization System

This section introduces the interactive visualization system within the print embodiment component.

A. System Overview

This system consists of three views, a print overview (Fig. 1(A)), an inspection view (Fig. 1(D)), and a detail view (Fig. 1(H)). We use blue hues, cyan hues, and orange hues to encode spatial features, kinematic features, and temporal features, respectively. The print overview visualizes all players' fingerprints with steerable glyphs (Fig. 1(B)). Analysts can adjust the glyph content on demand by using various filters and sliders. After selecting the fingerprint of interest, the inspection view presents detailed attention information on the four kinds of features (Fig. 1(F)). Analysts can inspect the differences in features between different players or tasks. In addition, analysts can further select the particular dimensions within each kind of feature to examine the raw biomechanical data in the detail view (Fig. 1(I)). The system is a web-based application. We used *React.js* to develop the frontend and the *Django* framework to develop the backend.

B. Print Overview

The print overview (Fig. 1(A)) contains two parts: fingerprint cards and a filter panel above the fingerprint cards.

1) Fingerprint Card: A fingerprint card (Fig. 1(B)) presents a player's fingerprint and his/her profile information. A new glyph is designed to encode a player's fingerprint. First, a ring is divided into three equal parts (120° each) to encode spatial features, kinematic features, and temporal features in blue, cyan, and orange, respectively (Fig. 5). Since each kind of feature

contains eight attention vectors, each arc is further divided into eight arcs and each arc encodes the value within an attention vector by a heat map (Fig. 5(B), (D), (E)). To facilitate the distinction of different features, the color hue of each heat map remains the same and the saturation is used to encode the value. The dimensions within an attention vector are grouped by using whitespace for better differentiation (Fig. 5(C)). For example, in Fig. 5(B), the arc presents the attention vector of the technique recognition model within spatial features. Most of the attention is paid to the racket and the left arm receives the least attention. In the center of the ring, a 32-dimensional radar chart is placed to display the summative features. The three sections of the radar chart corresponding to the three different features are encoded by the same color schemes for features Fig. 5(A). An alternative of the glyph is as Fig. 5(F) shows. The alternative unfolds the arc and encodes the summative attention with bar charts on the corresponding attention vectors. We did not adopt this design for two reasons. First, the alternative is too long to be perceived as a whole, unable to provide a holistic view of a fingerprint. Therefore, inspired by **DG10: Intuitive mapping based on semantics.** [5] and the design in Weng et al. [53], we used the metaphor of fingerprints and decided to use circular glyphs to augment the overall coherence. Second, since there are 32 attention vectors in a fingerprint, visualizing these vectors with heat maps horizontally makes it difficult to locate the same dimension of features among many fingerprints. Therefore, according to **DG5: Redundant mapping of variables.** in Borgo et al. [5], we use two visual channels, the position channel and the orientation channel to distinguish different features of different models in our glyph.

With the glyph, we place icons at the four corners of a card to encode a player's profile information (Fig. 1(B)). Starting from the top-left corner and moving clockwise, we have 1) an icon in the shape of a palm for the player's handedness (i.e., right palm: right-handedness, left palm: left-handedness), 2) a racket icon with different directions for the player's grip type (i.e., horizontal racket: shakehand grip, slanted racket: penhold grip), 3) the professional level abbreviations for the player's professional level (i.e., NL: national-level, L1: Level-1, L2: Level-2), and 4) a gender icon for the player's gender. For example, Fig. 1(B) presents the fingerprint card of a female right-handed player who uses a shakehand grip and is a Level-1 player.

Interactions: Analysts can click a group of arcs to select all corresponding features for further analysis. For example, if analysts select the arcs in Fig. 5(B), the arcs in Fig. 5(D) and 5(E) will also be selected and highlighted as Fig. 1(C) shows. The selected task of one player will be displayed in the inspection view.

2) Filter Panel: The filter panel at the top of this view enables analysts to adjust the glyphs of fingerprints from two perspectives. The filters in the first row support filtering based on model tasks. These filters can change the number of tangential arcs (Fig. 5(G)). The filters in the second row support filtering based on attention dimensions. These filters can change the number of radial arcs (Fig. 5(H)). Fig. 5(I) presents a fingerprint filtered by both kinds of filters.

Interations: All filters except for the slider support multiple selections. Analysts can select tasks and dimensions on demand. For the dimension filtering of temporal features, analysts can use the slider to choose the time period to be displayed in a fingerprint.

C. Inspection View

The inspection view (Fig. 1(D)) presents the details of the features selected in the print overview. For example, Fig. 1(F) presents the features selected in Fig. 1(C). Each kind of feature is presented with a separate visualization method. The details are as follows.

- *Summative charts* The summative feature is a three-dimensional vector. We use a pie chart to show the weight of the three kinds of features. The center of the pie chart is the model task. For example, the pie chart in Fig. 1(F) presents the summative features generated by the technique recognition model. It represents that the model pays the most attention to temporal features when recognizing Player 2's serve techniques.
- *Spatial charts* We use a bar chart with error bars to present the spatial feature. The lines with dark blue are the mean values and the rectangles indicate the standard confidence intervals. For example, in Fig. 1(F), the spatial feature indicates that the model pays the most attention to Player 2's racket.
- *Kinematic charts.* We use a similar visualization method to present the kinematic feature. For example, in Fig. 1(F), the kinematic feature indicates that the model pays the most attention to Player 2's magnetic field data, especially the z-axis.
- *Temporal chart.* We use a line chart with a confidence band inspired by Deng et al. [14] to present the temporal distribution of weights. For example, in Fig. 1(F), the two peaks indicate that most of the model's attention is focused on the middle period.

Interactions: Analysts can select two dimensions in the spatial chart or the kinematic chart to compare the raw data of the corresponding dimensions in the detail view (Fig. 1(H)). They can click on the corresponding bars in the charts and the chosen dimensions will be highlighted. For example, in Fig. 1(E) and (G), the right wrists within the spatial charts of Player 1 and Player 2 are selected.

D. Detail View

In the detail view (Fig. 1(H)), we show the biomechanical data of serves based on the time series. For example, Fig. 1(H) presents the biomechanical data of the right wrists of Player 1 and Player 4 (Fig. 1(E), (G)). Since there are many serves of a player, the data of each serve is not presented separately. We aggregate the data of serves with the same technique and placement by computing the mean value. Analysts can change the technique and placement by using the two buttons at the top of the detail view. By examining the biomechanical data, analysts can verify the findings in the inspection view.

TABLE III
THE MEAN AND STANDARD ERROR OF THE ACCURACY (10-FOLD) OF DIFFERENT MODELS DURING THE EXPERIMENT

Task name		BiLSTM	**BiLSTM-T**	BiLSTM-S	BiLSTM-K	LSTM	LightGBM	RF
Player	Avg.	**0.995**	0.990	0.984	0.985	0.965	0.994	0.993
	Std.	**0.003**	**0.003**	0.007	0.008	0.011	0.004	0.015
Gender	Avg.	0.996	**0.997**	0.995	0.994	0.978	0.921	0.989
	Std.	**0.002**	**0.002**	0.004	0.004	0.007	0.062	0.027
Profession	Avg.	**1.000**	**1.000**	**1.000**	0.999	0.977	0.993	0.994
	Std.	**0.000**	**0.000**	0.001	0.002	0.010	0.006	0.007
Grip	Avg.	0.994	**0.998**	0.995	0.992	0.963	0.974	0.963
	Std.	0.004	**0.002**	0.003	0.003	0.013	0.043	0.077
Technique	Avg.	**0.999**	0.997	0.995	0.995	0.959	0.955	0.958
	Std.	**0.002**	0.003	0.003	0.003	0.016	0.056	0.064
Spin	Avg.	0.944	**0.961**	0.946	0.930	0.817	0.733	0.577
	Std.	0.013	**0.008**	0.010	0.013	0.025	0.136	0.191
$Placement_h$	Avg.	0.566	**0.670**	0.629	0.628	0.496	0.381	0.459
	Std.	0.035	**0.014**	0.019	0.021	0.018	0.050	0.040
$Placement_v$	Avg.	0.948	**0.955**	0.951	0.924	0.753	0.895	0.813
	Std.	0.023	**0.011**	0.013	**0.011**	0.030	0.043	0.057

E. Usage Scenario

Here is a usage scenario where an analyst uses the system to compare the fingerprints between different players. He first examines the print overview (Fig. 1(A)). He browses the fingerprints of all players. He finds that the fingerprints of the players using penhold grip are quite different from those of the players using shakehand grip, especially in the spatial and kinematic features. To present the difference, he filters out several features that are similar among all fingerprints. Then, he selected features generated by the same model tasks from the fingerprints of three players. The details of the selected features are displayed in the inspection view (Fig. 1(D)). In the inspection view, he first examines the summative features to identify the most important feature types. He finds that the kinematic feature is the most important. He investigates the attention distribution within kinematic features by comparing the mean and confidence interval inside the chart of the kinematic feature. He selects one dimension in the charts of two players to observe the raw biomechanical data of the two players in the detail view (Fig. 1(H)). He examines the data of serves with different techniques and placements by using the filters at the top of the detail view. After checking the raw biomechanical data, he validated the differences in the fingerprints.

VI. EVALUATION

We designed a quantitative experiment to verify the model design in feature generation Fig. 3(B). In addition, we conducted a case study to evaluate the usability of the system. After the study, we interviewed the analysts about their feedback on the system. We also interviewed the players analyzed in the study for validation.

A. Model Evaluation

Apparatus: We compared our model (BiLSTM-T in Table III) with 6 alternatives. Wang et al. [49] have mentioned six advanced classification models (i.e., LSTM [22], Random Forest [41], Deep Forest [66], XGBoost [7], LightGBM [30]) for technique recognition. We added Random Forest, LSTM, and LightGBM to our alternative list. We removed Deep Forest since it is based on bootstrap aggregating, similar to Random Forest. Moreover, Random Forest performed better than it did in the previous study. Similarly, we selected LightGBM instead of XGBoost. Since our model is based on BiLSTM [19], we also added BiLSTM to the alternative list. In addition to the four alternatives, our model has another two alternatives, BiLSTM-S and BiLSTM-K. These two models have the same architecture as ours. The only difference is the key used to generate A_{SUM} in Fig. 4(F). Our model uses W_T, while BiLSTM-S uses W_S, and BiLSTM-K uses W_K.

Data: We recruited 12 professional players to collect the data for the experiment. Details can be referred to in Section III-C2. We set δ to 75 during data preparation (Section III-C3) since $150(2\delta)$ frames (Fig. 2(C)) are sufficient to encompass the data of a serve according to the previous work [49]. Totally, we used the data of 4319 serves.

Procedure & Result: We use 8 recognition tasks (Table III) to evaluate the performance of each model. To obtain a reliable evaluation result, we employed a 10-fold cross-validation method. We calculated the ratio of correctly recognized samples to the total number of samples as the accuracy. The mean and the standard error of accuracy are presented in Table III. According to the result, our model performed better than other models in recognizing horizontal ball positions ($Acc : 67\%, Std : 1.4\%$), vertical ball positions ($Acc : 95.5\%, Std : 1.1\%$), ball spin types ($Acc : 96.1\%, Std : 0.8\%$), grip styles ($Acc : 99.8\%, Std : 0.2\%$), and gender ($Acc : 99.7\%, Std : 0.2\%$). Especially when recognizing horizontal ball positions, our model performed much better than others. Besides, BiLSTM performed better than others in the tasks of recognizing serve techniques ($Acc : 99.9\%, Std : 0.2\%$) and players ($Acc : 99.5\%, Std : 0.3\%$). In addition, when recognizing levels of the profession, our model ($Acc : 100\%, Std : 0\%$) performed equivalently to the basic BiLSTM ($Acc : 100\%, Std : 0\%$). Therefore, in summary, the overall performance of our

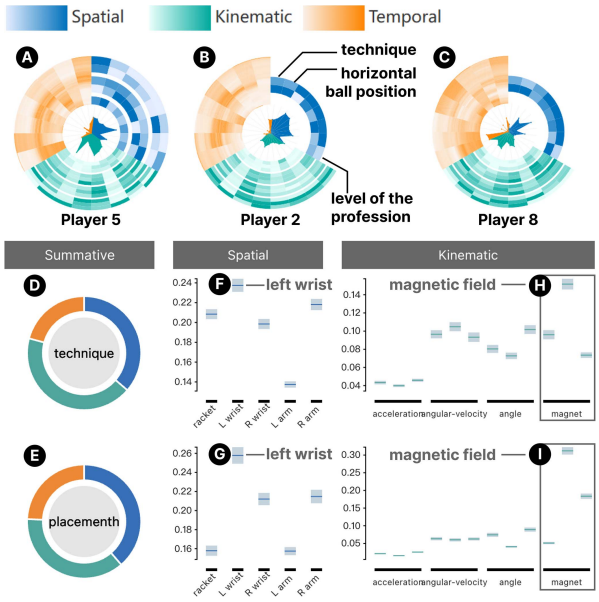

Fig. 6. Insight 1: (A) is the sound fingerprint of Player 2. (B) and (C) are filtered fingerprints of Player 5 and Player 8. (D)∼(I) displays the detailed information of the features generated by technique recognition and horizontal ball position recognition models of Player 5.

model is still relatively prominent. It can handle various recognition tasks.

B. Case Study

We conducted a case study with two analysts who have served the Chinese national table tennis team for more than three years. The data of the case study was the fingerprints of the 12 players we hired during data collection. We replaced the players' names with Player 1–12 to protect their privacy. We set δ to 75 to generate the fingerprints. We first introduced the visualizations and system interactions to the analysts. Then, we finished the case study together.

1) Insight 1. Redundant Movements on the Left Wrist: We first examined the fingerprints of all twelve players. According to the radar charts of each fingerprint, we found that the fingerprints of Player 2 and Player 5 were almost entirely focused on spatial features and kinematic features (Fig. 6(A), (b)). This indicates that the body coordination style (**R2**) and force style (**R3**) of these two players are the best representations of their biomechanical characteristics. However, their pace styles do not have any unique features since almost no attention to their temporal features. Therefore, we decided to focus on one of the two players, Player 2. We found that in the spatial features, the models' attention was basically focused on the left and right wrists of Player 2 in all of the model tasks (Fig. 6(B)). This aroused the curiosity of analysts. They wondered whether this pattern only occurred in Player 2's fingerprint. Therefore, we filtered out all other dimensions of the spatial features except for the two wrists by using the filters. We found that in addition to Player 2, Player 8 also had the same pattern (Fig. 6(C)). Analysts examined the profile information of the two players and found that they both used penhold grips, which was different from most of the other players. The analysts explained that this pattern is caused by the different playing styles of different grip types. Compared to players using shakehand grips, players using penhold grips had more movements on their right wrists when serving the ball with different techniques, ball positions, and spin types.

However, after we further examined the fingerprints of the two players, we found that the models' attention was not entirely paid to the right wrist. When recognizing serve techniques, horizontal ball positions, and levels of the profession, the attention was focused on the left wrist (Fig. 6(B)). Analysts said that generally speaking when a player changed his/her serve technique and ball position, the differences in his/her movements should be focused on the right wrist. The differences in movements of the left wrist should be relatively less. This was because the player needed to avoid unnecessary movements to confuse the opponent. However, the movements of the left wrist of these two players caught the attention of the model. Analysts concluded that the movements of these two players when serving the ball were not perfect enough. The left wrist had too many redundant movements which they needed to reduce during their training.

We further selected the spatial features generated by the technique recognition model and the horizontal ball position recognition model. In the inspection view, we found that both models indeed focused more on spatial and kinematic features according to the two donut charts (Fig. 6(D), (e)). In the spatial feature, attention to the left wrist was significantly higher than attention to other body joints, including the racket (Fig. 6(F), (G)). In the kinematic feature, attention to the magnetic field was significantly higher than attention to other kinematic indicators (Fig. 6(H), (I)). The analysts explained that changes in the magnetic field reflect changes in the range of the player's movements. The high attention indicated that Player 2's range of movements changed significantly when using different serve techniques, and these changes are reflected in the left wrist. To verify this conclusion, we selected the Y-axis of the magnetic field in both models to examine the raw biomechanical data of different body joints on the Y-axis of the magnetic field in the detail view. After we examined the data of different serve techniques and horizontal ball positions, we confirmed the analysts' reasoning.

2) Insight 2. Redundant Movements before/after Hitting: After investigating the spatial features and kinematic features, we decided to analyze the temporal features within fingerprints. We examined the temporal features of all players and found that players' temporal features are quite diverse. Therefore, the analysts suggested filtering out temporal features by tasks. We unselected the tasks unrelated to technical recognition in the filters. After filtering, we found that in most players' temporal features, the models' attention is mainly focused on the middle period of the serve process (Fig. 7(A)). This indicated that the biomechanical data during the period when the racket contacted the ball was the key for the model to distinguish different techniques and levels of the profession. The analysts stated that the players with this pattern must be high-level players because they do not conduct unnecessary movements at any time other than when hitting the ball.

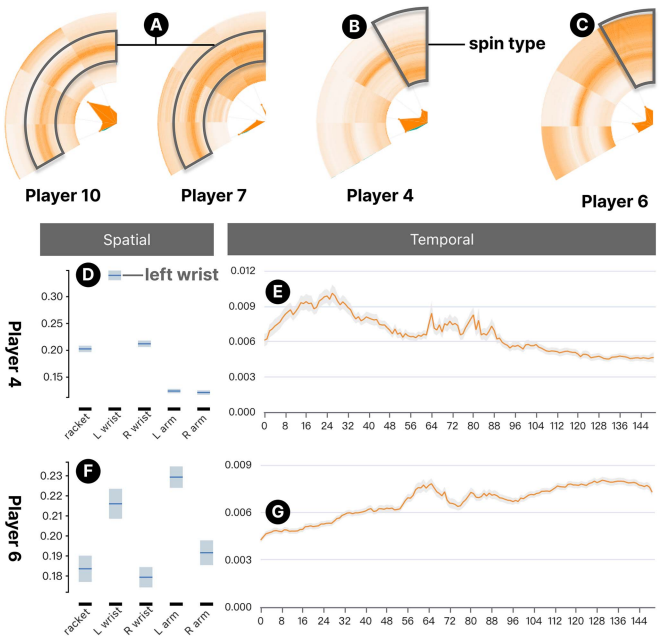

Fig. 7. Insight 2: (A), (B), and (C) present the temporal features of Player 7, 10, 4, and 6. (D), (E), (F), and (G) present the spatial features and temporal features generated by spin type recognition models of Player 4 and Player 6, respectively.

We also found some exceptions, such as Player 4 (Fig. 7(B)). The fingerprint of Player 4 shows that in the task of recognizing spin types, the model's attention mostly focused on the beginning of the serve process (the colors of the inner arcs are darker), which is the stage when the player tossed the ball. We selected this temporal feature and found a peak in the beginning of the serve in the inspection view (Fig. 7(E)). The analysts explained that the player's movements mainly changed before the ball was hit by the racket when serving with different spin types. Movements in this stage often had a subtle impact on the spin, as the spin was mainly determined by the contact between the racket and the ball. Therefore, it could be inferred that the quality of the spin of the player's serve was not high enough. In addition, the differences in movements during this stage could also provide hints for the opponent, allowing them to predict the spin type of the incoming serve in advance. This was an unfavorable condition for the player in a match. In the spatial feature, the model's attention focused on the left wrist (Fig. 7(D)), which was also unfavorable according to Insight 1.

Moreover, we found several examples where attention was concentrated on the latter half of the serve process. For instance, when the model recognized Player 6's spin types, the attention became more focused at the end of the serve process (Fig. 7(C)). We selected it, and in the inspection view, the line chart indeed presented a continuous upward trend (Fig. 7(G)). The analysts explained that the player's follow-through movements changed depending on the spin types of the ball. Such a situation was also unfavorable for a high-quality serve. Player 6 should improve it in subsequent training. We also found that the error bar of this player's spatial feature is quite long (Fig. 7(F)), indicating that the model's attention changes frequently when recognizing the player's spin types. This indirectly indicated that the coordination of the player's body joints was not very stable during each serve, which should be to be enhanced in terms of stability in future training.

C. Feedback

The analysts thought highly of the biomechanical fingerprints. We summarized their comments as follows.

- *Significance* This work introduces a novel method to generate the biomechanical fingerprints of table tennis players. The fingerprints can reflect players' habitual movement patterns which are important for skill improvement. Moreover, the fingerprint can enable coaches to discover players with similar/different playing styles, which can help create suitable matchups during training.
- *Embodiment* The visualization of fingerprints provides an efficient way for analysts to explore the fingerprint of each player. The use of the fingerprint metaphor vividly displays the uniqueness of each player as well as his/her similarities with others. The filters provide enough flexibility for analysts to adjust the presentation of the fingerprints on demand.
- *Data diversity* The diversity of the data used for fingerprint generation can be enlarged. In this work, all fingerprints were generated only based on serves. Although serves contain the most representative characteristics of a player, the fingerprint would be more comprehensive if it could include other strokes.

We present the insights in the case study to the corresponding players (i.e., Player 2, 4, 6). Player 2 admitted that he had some redundant movements on his left wrist. He was used to these movements and needed a long time to reduce such movements. Player 4 said when she used different spin types to serve, she would adopt different ways to toss the ball. This habit was difficult to change. Player 6 said she was not aware of her serve movements since her playing strategy did not require high-quality serves.

VII. Discussion

Application The biomechanical fingerprint of a player can play an important role in various situations. First, the fingerprint can help coaches discover the critical movements that influence players' performance during training. With this information, coaches can customize effective training plans for each player. Second, the fingerprint can help coaches identify talented players. Conventionally, coaches choose talented players based on their experience. Sometimes, it takes several rounds of training and matches. With the fingerprint, talented players can be easily detected since the coaches can clearly know the strengths and weaknesses of each player. If a player's fingerprint closely resembles that of top players, it indicates a significant potential for talent. Additionally, the fingerprint can also be used to construct virtual players in the metaverse for match simulation and prediction.

Generalizability TacPrint can be extended to a wide spectrum of sports (e.g., tennis, basketball, soccer) that involve diverse

movements and actions. First, we can bind IMU devices to the body parts involved in key technical movements to capture biomechanical data during training. For example, in soccer, the devices can be fixed on players' lower limbs to collect data during passing, shooting, dribbling, etc. In this step, challenges lie in the characterization of key technical movements representative body parts for data collection. Extensive collaboration with coaches and players and trial and error are necessary. Then, with the data, the model's recognition tasks can be tailored to the specific actions and player profiles involved in each sport. In this step, challenges lie in the model performance due to the variations in data size. For example, actions in basketball or soccer may involve longer durations and more complex movements compared to a serve in table tennis. Models should be refined based on specific sports. Finally, the fingerprints can be analyzed in the system by adjusting the icons on the fingerprint card. The icons should be redesigned according to the players' profile information in particular sports. For example, in basketball, we do not display a player's handedness and grip type. Instead, we may need to display his/her role (e.g., forward, guard) and height.

Limitation & future work This work has two limitations. First, the fingerprint is generated only based on the serve data. According to the analysts, other strokes besides the serve are also valuable when describing players' characteristics. In the future, we will combine the data of other strokes to enrich the fingerprint. Second, the device can influence players' performance due to its size and weight. In the future, we need unobtrusive wearable devices to reduce the influence. Moreover, if we combine other types of strokes into the fingerprint, more devices should be prepared to collect the movements of other body joints such as ankles, knees, and legs.

Reflection We added the attention mechanism to enhance the model interpretability. However, domain experts still have difficulties understanding the attention vectors of the models due to their abstract definitions and complicated calculation methods. Therefore, visualization is indispensable in promoting the application of machine learning models in various fields. However, complex visualizations would increase experts' learning curves, eliminating the convenience brought by visualization. Therefore, we used basic visualization methods to construct the new glyph of the fingerprint and display the details of different types of features, facilitating experts' understanding.

VIII. Conclusion

In this work, we proposed the definition of the biomechanical fingerprint and developed a framework, TacPrint to help the experts generate and analyze players' fingerprints. TacPrint takes the biomechanical data collected by IMU devices as input and generates spatial features, kinematic features, and temporal features of a fingerprint by using the BiLSTM network with attention layers. We further designed a novel glyph and developed an interactive system to support the exploration of the fingerprints. With the system, we conducted a case study based on table tennis data and discovered valuable insights about players' performance enhancement during the training. In addition to table tennis, TacPrint can also be extended to other sports such as tennis and basketball to help improve players' performance, prevent potential injuries, identify talents, and develop personalized training programs. In the future, We will continue to explore the generalizability of TacPrint in other sports and biomechanical analysis fields.

References

[1] G. Andrienko et al., "Visual analysis of pressure in football," *Data Mining Knowl. Discov.*, vol. 31, pp. 1793–1839, 2017, doi: 10.1007/s10618–017-0513-2.

[2] J. Bernard, A. Vögele, R. Klein, and D. W. Fellner, "Approaches and challenges in the visual-interactive comparison of human motion data," in *Proc. Int. Joint Conf. Comput. Vis. Imag. Comput. Graph. Theory Appl.*, 2017, pp. 217–224, doi: 10.5220/0006127502170224.

[3] P. Blank, B. H. Groh, and B. M. Eskofier, "Ball speed and spin estimation in table tennis using a racket-mounted inertial sensor," in *Proc. ACM Int. Symp. Wearable Comput.*, 2017, pp. 2–9, doi: 10.1145/3123021.3123040.

[4] P. Blank, J. Hoßbach, D. Schuldhaus, and B. M. Eskofier, "Sensor-based stroke detection and stroke type classification in table tennis," in *Proc. ACM Int. Symp. Wearable Comput.*, 2015, pp. 93–100, doi: 10.1145/2802083.2802087.

[5] R. Borgo et al., "Glyph-based visualization: Foundations, design guidelines, techniques and applications," in *Proc. Eurographics*, 2013, pp. 39–63, doi: 10.2312/conf/EG2013/stars/039–063.

[6] L. Breiman, "Random forests," *Mach. Learn.*, vol. 45, pp. 5–32, 2001, doi: 10.1023/A1010933404324.

[7] T. Chen and C. Guestrin, "XGBoost: A scalable tree boosting system," in *Proc. Int. Conf. Knowl. Discov. Data Mining*, 2016, pp. 785–794, doi: 10.1145/2939672.2939785.

[8] W. Chen et al., "GameFlow: Narrative visualization of NBA basketball games," *IEEE Trans. Multimedia*, vol. 18, no. 11, pp. 2247–2256, Nov. 2016, doi: 10.1109/TMM.2016.2614221.

[9] Z. Chen et al., "Sporthesia: Augmenting sports videos using natural language," *IEEE Trans. Vis. Comput. Graph.*, vol. 29, no. 1, pp. 918–928, Jan. 2023, doi: 10.1109/TVCG.2022.3209497.

[10] D. H. S. Chung et al., "Glyph sorting: Interactive visualization for multi-dimensional data," *Inf. Visual.*, vol. 14, no. 1, pp. 76–90, 2015, doi: 10.1177/1473871613511959.

[11] D. H. S. Chung et al., "Knowledge-assisted ranking: A visual analytic application for sports event data," *IEEE Comput. Graph. Appl.*, vol. 36, no. 3, pp. 72–82, May/Jun. 2016, doi: 10.1109/MCG.2015.25.

[12] D. Deng, A. Wu, H. Qu, and Y. Wu, "DashBot: Insight-driven dashboard generation based on deep reinforcement learning," *IEEE Trans. Vis. Comput. Graph.*, vol. 29, no. 1, pp. 690–700, Jan. 2023, doi: 10.1109/TVCG.2022.3209468.

[13] D. Deng et al., "VisImages: A fine-grained expert-annotated visualization dataset," *IEEE Trans. Vis. Comput. Graph.*, vol. 29, no. 7, pp. 3298–3311, Jul. 2023, doi: 10.1109/TVCG.2022.3155440.

[14] Z. Deng et al., "Visualizing large-scale spatial time series with geoChron," *IEEE Trans. Vis. Comput. Graph.*, vol. 30, no. 1, pp. 1194–1204, Jan. 2024, doi: 10.1109/TVCG.2023.3327162.

[15] M. Du and X. Yuan, "A survey of competitive sports data visualization and visual analysis," *J. Visual.*, vol. 24, no. 1, pp. 47–67, 2020, doi: 10.1007/s12650–020-00687-2.

[16] F. Fu, Y. Zhang, S. Shao, J. Ren, M. Lake, and Y. Gu, "Comparison of center of pressure trajectory characteristics in table tennis during topspin forehand loop between superior and intermediate players," *Int. J. Sports Sci. Coaching*, vol. 11, no. 4, pp. 559–565, 2016, doi: 10.1177/1747954116654778.

[17] K. Goldsberry, "Courtvision: New visual and spatial analytics for the NBA," in *Proc. MIT Sloan Sports Analytics Conf.*, 2012, pp. 12–15.

[18] F. Gravenhorst, A. Muaremi, C. Draper, M. Galloway, and G. Tröster, "Identifying unique biomechanical fingerprints for rowers and correlations with boat speed-a data-driven approach for rowing performance analysis," *Int. J. Comput. Sci. Sport*, vol. 14, no. 1, pp. 4–33, 2015.

[19] A. Graves, A.-R. Mohamed, and G. Hinton, "Speech recognition with deep recurrent neural networks," in *Proc. IEEE Int. Conf. Acoust. Speech Signal Process.*, 2013, pp. 6645–6649, doi: 10.1109/ICASSP.2013.6638947.

[20] Y. He, G. Fekete, D. Sun, J. S. Baker, S. Shao, and Y. Gu, "Lower limb biomechanics during the topspin forehand in table tennis: A systemic review," *Bioengineering*, vol. 9, no. 8, 2022, Art. no. 336, doi: 10.3390/bioengineering9080336.

[21] M. A. Hearst, S. T. Dumais, E. Osuna, J. Platt, and B. Scholkopf, "Support vector machines," *IEEE Intell. Syst. Their Appl.*, vol. 13, no. 4, pp. 18–28, Jul./Aug. 1998, doi: 10.1109/5254.708428.

[22] S. Hochreiter and J. Schmidhuber, "Long short-term memory," *Neural Computation*, vol. 9, no. 8, pp. 1735–1780, 1997, doi: 10.1162/neco.1997.9.8.1735.

[23] N. Ibrahim, N. A. Abu Osman, A. H. Mokhtar, N. Arifin, J. Usman, and H. N. Shasmin, "Contribution of the arm segment rotations towards the horizontal ball and racket head velocities during forehand long shot and drop shot services in table tennis," *Sports Biomech.*, vol. 21, no. 9, pp. 1065–1081, 2022, doi: 10.1080/14763141.2020.1726995.

[24] Y. Iino and T. Kojima, "Kinematics of table tennis topspin forehands: Effects of performance level and ball spin," *J. Sports Sci.*, vol. 27, no. 12, pp. 1311–1321, 2009, doi: 10.1080/02640410903264458.

[25] Y. Iino and T. Kojima, "Kinetics of the upper limb during table tennis topspin forehands in advanced and intermediate players," *Sports Biomech.*, vol. 10, no. 4, pp. 361–377, 2011, doi: 10.1080/14763141.2011.629304.

[26] Y. Iino and T. Kojima, "Effect of the racket mass and the rate of strokes on kinematics and kinetics in the table tennis topspin backhand," *J. Sports Sci.*, vol. 34, no. 8, pp. 721–729, 2016, doi: 10.1080/02640414.2015.1069377.

[27] Y. Iino, S. Yoshioka, and S. Fukashiro, "Uncontrolled manifold analysis of joint angle variability during table tennis forehand," *Hum. Movement Sci.*, vol. 56, pp. 98–108, 2017, doi: 10.1016/j.humov.2017.10.021.

[28] Y. Iino, S. Yoshioka, and S. Fukashiro, "Effect of mechanical properties of the lower limb muscles on muscular effort during table tennis forehand," *ISBS Proc. Arch.*, vol. 36, no. 1, 2018, Art. no. 770.

[29] H. Janetzko, D. Sacha, M. Stein, T. Schreck, D. A. Keim, and O. Deussen, "Feature-driven visual analytics of soccer data," in *Proc. IEEE Conf. Vis. Analytics Sci. Technol.*, 2014, pp. 13–22, doi: 10.1109/VAST.2014.7042477.

[30] G. Ke et al., "LightGBM: A highly efficient gradient boosting decision tree," in *Proc. Adv. Neural Inf. Process. Syst.*, 2017, pp. 3146–3154, doi: 10.5555/3294996.3295074.

[31] W.-K. Lam, J.-X. Fan, Y. Zheng, and W. C.-C. Lee, "Joint and plantar loading in table tennis topspin forehand with different footwork," *Eur. J. sport Sci.*, vol. 19, no. 4, pp. 471–479, 2019, doi: 10.1080/17461391.2018.1534993.

[32] A. Lees, "Science and the major racket sports: A review," *J. Sports Sci.*, vol. 21, no. 9, pp. 707–732, 2003, doi: 10.1080/0264041031000140275.

[33] P. A. Legg et al., "Transformation of an uncertain video search pipeline to a sketch-based visual analytics loop," *IEEE Trans. Vis. Comput. Graph.*, vol. 19, no. 12, pp. 2109–2118, Dec. 2013, doi: 10.1109/TVCG.2013.207.

[34] P. A. Legg et al., "MatchPad: Interactive glyph-based visualization for real-time sports performance analysis," *Comput. Graph. Forum*, vol. 31, no. 3, pp. 1255–1264, 2012, doi: 10.1111/j.1467–8659.2012.03118.x.

[35] G. Letarte, F. Paradis, P. Giguére, and F. Laviolette, "Importance of self-attention for sentiment analysis," in *Proc. EMNLP Workshop BlackboxNLP: Analyzing Interpreting Neural Netw. NLP*, 2018, pp. 267–275, doi: 10.18653/v1/W18–5429.

[36] T. Lin, Z. Chen, Y. Yang, D. Chiappalupi, J. Beyer, and H. Pfister, "The quest for : Embedded visualization for augmenting basketball game viewing experiences," *IEEE Trans. Vis. Comput. Graph.*, vol. 29, no. 1, pp. 962–971, Jan. 2023, doi: 10.1109/TVCG.2022.3209353.

[37] S. Lu, X. Zhang, J. Wang, Y. Wang, M. Fan, and Y. Zhou, "An IoT-Based motion tracking system for next-generation foot-related sports training and talent selection," *J. Healthcare Eng.*, 2021, 2021, Art. no. 9958256, doi: 10.1155/2021/9958256.

[38] R. Ma et al., "Basketball movements recognition using a wrist wearable inertial measurement unit," in *Proc. IEEE Int. Conf. Micro/Nano Sensors AI Healthcare Robot.*, 2018, pp. 73–76, doi: 10.1109/NSENS.2018.8713634.

[39] T. Mitsui, S. Tang, and S. Obana, "Support system for improving golf swing by using wearable sensors," in *Proc. Eighth Int. Conf. Mobile Comput. Ubiquitous Netw.*, 2015, pp. 100–101, doi: 10.1109/ICMU.2015.7061049.

[40] Z. Niu, G. Zhong, and H. Yu, "A review on the attention mechanism of deep learning," *Neurocomputing*, vol. 452, pp. 48–62, 2021, doi: 10.1016/j.neucom.2021.03.091.

[41] F. Pedregosa et al., "Scikit-learn: Machine learning in python," *J. Mach. Learn. Res.*, vol. 12, pp. 2825–2830, 2011, doi: 10.5555/1953048.2078195.

[42] C. Perin, J. Boy, and F. Vernier, "Using gap charts to visualize the temporal evolution of ranks and scores," *IEEE Comput. Graph. Appl.*, vol. 36, no. 5, pp. 38–49, Sep./Oct. 2016, doi: 10.1109/MCG.2016.100.

[43] C. Perin, R. Vuillemot, C. D. Stolper, J. T. Stasko, J. Wood, and S. Carpendale, "State of the art of sports data visualization," *Comput. Graph. Forum*, vol. 37, no. 3, pp. 663–686, 2018, doi: 10.1111/cgf.13447.

[44] T. Polk, J. Yang, Y. Hu, and Y. Zhao, "TenniVis: Visualization for tennis match analysis," *IEEE Trans. Vis. Comput. Graph.*, vol. 20, no. 12, pp. 2339–2348, Dec. 2014, doi: 10.1109/TVCG.2014.2346445.

[45] A. Rusu, D. Stoica, E. Burns, B. Hample, K. McGarry, and R. Russell, "Dynamic visualizations for soccer statistical analysis," in *Proc. 14th Int. Conf. Inf. Visualisation*, 2010, pp. 207–212, doi: 10.1109/IV.2010.39.

[46] R. Sisneros and M. Van Moer, "Expanding plus-minus for visual and statistical analysis of NBA box-score data," in *Proc. 1st Workshop Sports Data Visual.*, 2013.

[47] M. Stein, J. Häußler, D. Jäckle, H. Janetzko, T. Schreck, and D. A. Keim, "Visual soccer analytics: Understanding the characteristics of collective team movement based on feature-driven analysis and abstraction," *ISPRS Int. J. Geo- Inf.*, vol. 4, no. 4, pp. 2159–2184, 2015, doi: 10.3390/ijgi4042159.

[48] M. Stein et al., "Bring it to the pitch: Combining video and movement data to enhance team sport analysis," *IEEE Trans. Vis. Comput. Graph.*, vol. 24, no. 1, pp. 13–22, Jan. 2018, doi: 10.1109/TVCG.2017.2745181.

[49] J. Wang et al., "Tac-Trainer A: Visual analytics system for IoT-Based racket sports training," *IEEE Trans. Vis. Comput. Graph.*, vol. 29, no. 1, pp. 951–961, Jan. 2023, doi: 10.1109/TVCG.2022.3209352.

[50] J. Wang et al., "Tac-miner: Visual tactic mining for multiple table tennis matches," *IEEE Trans. Vis. Comput. Graph.*, vol. 27, no. 6, pp. 2770–2782, 2021, doi: 10.1109/TVCG.2021.3074576.

[51] J. Wang et al., "Tac-Simur: Tactic-based simulative visual analytics of table tennis," *IEEE Trans. Vis. Comput. Graph.*, vol. 26, no. 1, pp. 407–417, Jan. 2020, doi: 10.1109/TVCG.2019.2934630.

[52] Y. Wang, M. Chen, X. Wang, R. H. M. Chan, and W. J. Li, "IoT for next-generation racket sports training," *IEEE Internet Things J.*, vol. 5, no. 6, pp. 4558–4566, Dec. 2018, doi: 10.1109/JIOT.2018.2837347.

[53] D. Weng et al., "Towards better bus networks: A visual analytics approach," *IEEE Trans. Vis. Comput. Graph.*, vol. 27, no. 2, pp. 817–827, Feb. 2021, doi: 10.1109/TVCG.2020.3030458.

[54] S. Wiegreffe and Y. Pinter, "Attention is not not explanation," in *Proc. Conf. Empirical Methods Natural Lang. Process., 9th Int. Joint Conf. Natural Lang. Process.*, 2019, , pp. 11–20, doi: 10.48550/arXiv.1908.04626.

[55] D. W.-C. Wong, W. C.-C. Lee, and G. W. K. Lam, "Biomechanics of table tennis: A systematic scoping review of playing levels and maneuvers," *Appl. Sci.*, vol. 10, no. 15, 2020, Art. no. 5203, doi: 10.3390/app10155203.

[56] K. Wongsuphasawat and D. Gotz, "Exploring flow, factors, and outcomes of temporal event sequences with the outflow visualization," *IEEE Trans. Vis. Comput. Graph.*, vol. 18, no. 12, pp. 2659–2668, Dec. 2012, doi: 10.1109/TVCG.2012.225.

[57] J. Wu, D. Liu, Z. Guo, and Y. Wu, "RASIPAM: Interactive pattern mining of multivariate event sequences in racket sports," *IEEE Trans. Vis. Comput. Graph.*, vol. 29, no. 1, pp. 940–950, Jan. 2023, doi: 10.1109/TVCG.2022.3209452.

[58] J. Wu, D. Liu, Z. Guo, Q. Xu, and Y. Wu, "TacticFlow: Visual analytics of ever-changing tactics in racket sports," *IEEE Trans. Vis. Comput. Graph.*, vol. 28, no. 1, pp. 835–845, Jan. 2022, doi: 10.1109/TVCG.2021.3114832.

[59] Y. Wu et al., "OBTracker: Visual analytics of off-ball movements in basketball," *IEEE Trans. Vis. Comput. Graph.*, vol. 29, no. 1, pp. 929–939, Jan. 2023, doi: 10.1109/TVCG.2022.3209373.

[60] Y. Wu et al., "iTTVis: Interactive visualization of table tennis data," *IEEE Trans. Vis. Comput. Graph.*, vol. 24, no. 1, pp. 709–718, Jan. 2018, doi: 10.1109/TVCG.2017.2744218.

[61] K. Xia, H. Wang, M. Xu, Z. Li, S. He, and Y. Tang, "Racquet sports recognition using a hybrid clustering model learned from integrated wearable sensor," *Sensors*, vol. 20, no. 6, pp. 1638, 2020, doi: 10.3390/s20061638.

[62] X. Xie et al., "Passvizor: Toward better understanding of the dynamics of soccer passes," *IEEE Trans. Vis. Comput. Graph.*, vol. 27, no. 2, pp. 1322–1331, Feb. 2021, doi: 10.1109/TVCG.2020.3030359.

[63] W. Yang, M. Liu, Z. Wang, and S. Liu, "Foundation models meet visualizations: Challenges and opportunities," *Comput. Vis. Media*, 2024.

[64] L. Yao, A. Bezerianos, R. Vuillemot, and P. Isenberg, "Visualization in motion: A research agenda and two evaluations," *IEEE Trans. Vis. Comput. Graph.*, vol. 28, no. 10, pp. 3546–3562, Oct. 2022, doi: 10.1109/TVCG.2022.3184993.

[65] C. Yu, S. Shao, J. S. Baker, and Y. Gu, "Comparing the biomechanical characteristics between squat and standing serves in female table tennis athletes," *PeerJ*, vol. 6, 2018, Art. no. e4760, doi: 10.7717/peerj.4760.

[66] Z. Zhou and J. Feng, "Deep forest: Towards an alternative to deep neural networks," in *Proc. Int. Joint Conf. Artif. Intell.*, 2017, pp. 3553–3559, doi: 10.24963/ijcai.2017/497.